Luo *et al. Int J Concr Struct Mater* (2022) 16:9
https://doi.org/10.1186/s40069-022-00503-1

International Journal of Concrete Structures and Materials

RESEARCH Open Access

# Carbonation Model and Prediction of Polyvinyl Alcohol Fiber Concrete with Fiber Length and Content Effects

Zuyun Luo[1,2], Xinhua Yang[1*], Heli Ji[1] and Chuanchuan Zhang[3]

**Abstract**

Durability is an important aspect of reliability of concrete structures. In order to establish the carbonation model of polyvinyl alcohol (PVA) fiber concrete including the influences of PVA fiber length and volume content, a series of accelerated carbonation experiments were carried out on the normal concrete specimens and PVA fiber concrete specimens with fiber lengths of 3 mm, 6 mm, 12 mm and 18 mm and fiber volume contents of 0.1%, 0.3%, 0.5%, 0.75%, 1.0% and 1.5%, respectively. The experimental conditions remained at temperature of 20 ℃, humidity of 70%, and carbon dioxide concentration of 20%. It was found that the addition of PVA fibers could improve the carbonation resistance of concrete considerably. Within the investigated range of fiber length and content, the carbonation resistance of concrete is first strengthened and then weakened with increasing PVA fiber length or content. The quadratic carbonation depth prediction model could characterize the influences of PVA fiber length and content better than the linear model. The carbon dioxide diffusion equation was established by introducing a PVA fiber influence factor and its parameters were determined from the carbonation depth prediction model. The carbonation process of PVA fiber concrete under the accelerated carbonation experiment condition was simulated. Both the model and the numerical method were validated by comparison between the experimental and numerical results. Finally, the influences of added PVA fibers on the carbonation life and durability of reinforced concrete components were further studied numerically. The results showed that compared with the normal concrete component, the durability of PVA fiber concrete components is significantly improved.

**Keywords:** polyvinyl alcohol fiber, concrete, accelerated carbonation experiment, carbonation model

## 1 Introduction

As one of the most widely used construction and building materials, concrete has high compressive strength, but low tensile and bending strength, poor ductility, and low fracture toughness (An et al., 2014; Pacheco-Torgal et al., 2012; Samarakkody et al., 2017). In order to improve the mechanical properties, various kinds of fibers, such as steel fibers (Belletti et al., 2008; Fuente et al., 2012; Tiberti et al., 2018), jute fibers (Razmi & Mirsayar, 2017), carbon fibers (Spelter et al., 2019), polyvinyl alcohol (PVA) fibers (Zhang & Yang, 2019), etc., have been added into concrete. They can effectively inhibit the initiation and development of micro-cracks in the early hardening process of concrete, and bring better tensile, bending and crack-control properties to concrete. Steel fiber concrete received attention first. However, it has non-ignorable downsides, such as increased concrete density and non-uniform distribution of fibers in concrete, as well as steel fiber corrosion. In recent years, synthetic fibers, such as PVA fibers, attracted wide attention due to their high acid and alkaline resistance, high bonding strength with the cement matrix, and relatively low cost. At present,

*Correspondence: yangxinh@hust.edu.cn
[1] School of Aerospace Engineering, Huazhong University of Science and Technology, Wuhan 430074, China
Full list of author information is available at the end of the article
Journal information: ISSN 1976-0485 / eISSN 2234-1315

PVA fiber concrete has been applied in some engineering practices (Muntean et al., 2017; Thong et al., 2016; Zhu & Lv, 2011).

With the increasing attention paid to the durability of concrete, the carbonation resistance of concrete, as one of the most important aspects of the durability problem, has become a hot issue of research and attention (Chen & Qian, 2017; Ding & Chen, 2019; Frazão et al., 2015; Possan et al., 2016). Carbon dioxide in the environment intrudes into porous concrete and dissolves in the pore solution to form carbonic acid, which reacts with the calcium hydroxide around the pores to form calcium carbonate (Mi et al., 2019; Omikrine Metalssi et al., 2020). This reaction continues until the pH value in the pore solution drops to the range of 8.5 ~ 9.0. Therefore, the carbonation is a process that develops slowly from the surface to the inside of concrete. In reinforced concrete structures, once concrete carbonation passes through the protective layer, the depassivation of the internal reinforcement would occur (Carević & Ignjatović, 2019; Han et al., 2016; Saetta et al., 1993; WSNB Dong Cui, 2018).

In recent decades, the research on the prediction model of concrete carbonation depth attracted much attention. For example, in 2020, Liu et al. (2020) studied the carbonation rate of concrete in different environments, and proposed a carbonation depth prediction model considering the effects of temperature, relative humidity and carbon dioxide concentration. Felix et al. (2021) established a carbonation model for fly ash concrete based on the artificial neural network, and evaluated the effects of the cement consumption and fly ash content, as well as carbon dioxide concentration and relative humidity. Li et al. (2020) proposed three mathematical models to describe the diffusion of carbon dioxide in concrete with different carbonation reaction rates, respectively.

Some attention was also paid to synthetic fiber modified concrete. Flores Medina et al. (2014, 2015) studied the effects of polypropylene (PP) fibers on early age shrinkage and cracking in the concrete with natural pozzolan cement and their combined influences with silica fume on concrete durability. Tonoli et al. (Tonoli et al., 2019) showed the effects of the initial moisture content on the carbonation degree, mechanical and physical properties of fiber–cement composites after their exposition to carbon dioxide atmosphere and after accelerated ageing cycles. Zhang et al. (2018) investigated the carbonation durability of engineered cementitious composites and concluded that the material reinforced with 2 vol % PP fibers has superior carbonized durability. Up to now, however, no quantitative prediction model is given for carbonation depth prediction of synthetic fiber modified concrete.

In this paper, some rapid carbonation experiments were performed on the normal concrete and PVA fiber concrete specimens, and the influences of PVA fiber length and content on the concrete carbonation are studied to establish the carbonation model of PVA fiber concrete including the influences of PVA fiber length and volume content. Finally, as a simple application, the model was used to numerically evaluate the durability of reinforced PVA fiber concrete components after validation.

## 2 Experimental Method

### 2.1 Materials

P.I.42.5 Portland cement, medium sand, continuous graded coarse limestone aggregates with density of 2719 $kg{\cdot}m^{-3}$, tap water, and PVA fibers with lengths of 3 mm, 6 mm, 12 mm and 18 mm (see Fig. 1 for 6 mm and 18 mm) were used as raw materials to prepare specimens. The chemical composition of Portland cement, the physical and mechanical properties of PVA fibers, the aggregate gradation, and the concrete mix proportions are shown in Tables 1, 2, 3, 4, respectively.

### 2.2 Experimental Procedures

The specimens have sizes of 100 mm × 100 mm × 100 mm. They are divided into two kinds: one is normal concrete specimens with zero PVA fiber content, and the other is PVA fiber concrete specimens with different fiber lengths and contents. Except for the normal concrete specimens, there are 18 combinations of fiber length and content in total. Among them, the specimens with fiber lengths of 6 mm and 12 mm have fiber contents of 0.1%, 0.3%, 0.5%, 0.75%, 1% and 1.5%, respectively, but the specimens with fiber lengths of 3 mm and 18 mm have only fiber contents of 0.1%, 0.3% and 0.5%, respectively, as shown in Table 5. Each combination of PVA fiber length and content, including normal concrete without PVA fiber, has 12 specimens, every three ones of which are for the 7-, 14-, 21- and 28-day carbonation experiments, respectively.

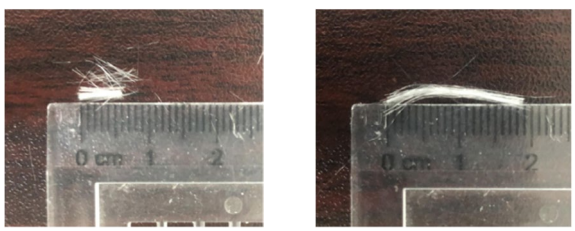

(a) 6 mm (b) 18 mm

**Fig. 1** PVA fibers of different lengths.

**Table 1** Chemical composition of Portland cement.

| Composition | $SiO_2$ | $Al_2O_3$ | $Fe_2O_3$ | CaO | MgO | $R_2O$ | LOI |
|---|---|---|---|---|---|---|---|
| Content /% | 20.6 | 5.0 | 3.4 | 63.3 | 1.3 | 0.5 | 1.76 |

LOI is the loss on ignition, namely the percentage of weight lost after ignition between 1000 and 1100 °C

**Table 2** Physical and mechanical properties of PVA fibers.

| Diameter /μm | Elongation at break /% | Tensile strength / MPa | Initial modulus / GPa | Density/$g/cm^2$ |
|---|---|---|---|---|
| 15 | 6.9 | 1830 | 40 | 1.29 |

**Table 3** Aggregate gradation.

| Grain size / mm | Sieving size / mm | Sieving mass / kg | Mass content /% | Passing rate /% |
|---|---|---|---|---|
| 0–4.75 | 4.75 | 193 | 3.86 | 3.86 |
| 4.75–9.5 | 9.5 | 1678 | 33.57 | 37.43 |
| 9.5–16.0 | 16.0 | 2108 | 42.18 | 79.61 |
| 16.0–19.0 | 19.0 | 652 | 13.05 | 92.66 |
| 19.0–26.5 | 26.5 | 367 | 7.34 | 100.00 |

**Table 4** Concrete mix proportions.

| Cement /kg $m^{-3}$ | Sand /kg $m^{-3}$ | Aggregates /kg $m^{-3}$ | Water /kg $m^{-3}$ |
|---|---|---|---|
| 433 | 674 | 1148 | 195 |

In accordance with the state standard of the People's Republic of China (GBT50082-2009) (The state standard of the People's Republic of China, 2009), after curing and demolding, the specimens were put into the standard curing room with temperature of 20 °C and relative humidity of 95% above for 28 days. After that, they were put into the drying oven and dried at 60 °C for 48 h to fully dissipate the water inside the specimens. Finally, they were cooled naturally. For the carbonation experiments, two opposite sides of each specimen were retained, but the remaining surfaces were sealed with paraffin wax.

After the preparations have been made, all the specimens were put into the accelerated carbonation chamber to carry out the accelerated carbonation experiments. The experimental temperature was controlled at 20 ± 3 °C, the humidity was 70 ± 5%, and the carbon dioxide concentration was 20 ± 5%. Three specimens in each combination were taken out when the carbonation time reaches 7, 14, 21 and 28 days, respectively. Measuring points were set every 10 mm interval on the retained surfaces of each specimen, as shown in Fig. 2a. Then the specimens were cut up at every measuring point and then 1% phenolphthalein alcohol solution was sprayed to the cutting surfaces, as shown in Fig. 2b. Finally, the distance of the color boundary from the specimen surface was measured as the carbonation depth at the corresponding measuring point, as shown in Fig. 2c. The arithmetic averages of carbonation depth were computed for all measuring points of each specimen and for all specimens of each combination. The data from the normal concrete specimens were treated as the reference.

## 3 Effects of PVA Fiber Length and Content on Carbonation

### 3.1 Prediction Model of Carbonation Depth

In order to study the fiber content effect on the carbonation, the fiber length was fixed on 6 mm and 12 mm, respectively, but the fiber content was changed from 0.1 to 0.3%, 0.5%, 0.75%, 1%, and 1.5%. Fig. 3 shows the variation of carbonation depth versus time for the PVA fiber concrete specimens with fiber lengths of 6 mm and 12 mm and different fiber contents. For comparison, the carbonation data of normal concrete specimens are also

**Table 5** Combination of PVA fiber length and content.

| Fiber length | Fiber content | | | | | |
|---|---|---|---|---|---|---|
| | 0.1 | 0.3 | 0.5 | 0.75 | 1 | 1.5 |
| 3 mm | √ | √ | √ | | | |
| 6 mm | √ | √ | √ | √ | √ | √ |
| 12 mm | √ | √ | √ | √ | √ | √ |
| 18 mm | √ | √ | √ | | | |

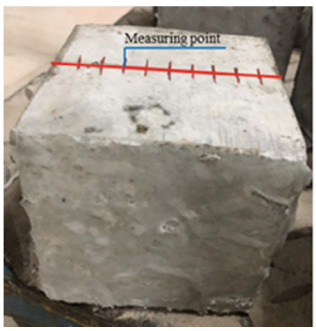


(a) Measuring point distribution

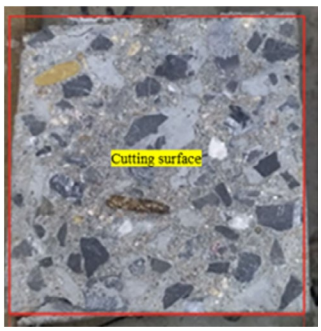


(b) Cutting surface at a measuring point

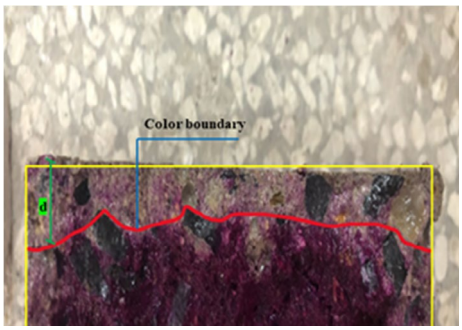


(c) Carbonization depth measurement

**Fig. 2** Main steps of carbonization depth measurement.

plotted in it. It can be seen that the carbonation depth has a decreasing growth rate with time, which is very consistent with Fick's second law. Accordingly, similar to the normal concrete, the carbonation depth of the PVA fiber concrete can be assumed to be directly proportional to the square root of time. In addition, for the same fiber length and carbonation time, the carbonation depth first decreases with the PVA fiber content increasing from 0 to 0.75%, and then increases with the increase of PVA fiber content from 0.75 to 1.5%. Therefore, no matter the length of PVA fiber is 6 mm or 12 mm, for the same carbonation time, the carbonation depth of PVA fiber concrete with 0.75% content is the minimum. It indicates that PVA fiber concrete with 0.75% content has the strongest carbonation resistance.

This is because the incorporation of appropriate amount of PVA fibers into concrete can improve the internal structure and reduce the porosity, thus improving the compactness and the resistance of carbon dioxide penetration (Aminul Haque et al., 2019). In addition, the incorporation of PVA fibers can also inhibit the formation and development of early cracks as channels for the diffusion of carbon dioxide in concrete (Chen et al., 2018, 2019; Li & Cao, 2018). However, if too many fibers are added, they would cluster around each other, so that the fibers cannot fully integrate with concrete and there is a negative impact on the hydration process of concrete (Xu et al., 2020). Moreover, the clustering of fibers can also produce voids inside the concrete to accelerate the penetration of carbon dioxide. Additionally, it is worth pointing out that, compared with the normal concrete specimen, the PVA fiber concrete specimens have worse fluidity and a less slump, but stronger adhesion during the concrete-making process.

In order to study the fiber length effect on carbonation, the fiber content was fixed on 0.1%, 0.3%, and 0.5%, respectively, but the fiber length was changed from 3 to 6 mm, 12 mm and 18 mm. Fig. 4 shows the variation of carbonation depth versus time for the PVA fiber concrete specimens with fiber contents of 0.1%, 0.3%, and 0.5% and different fiber lengths, respectively. It can be seen that when the fiber content is 0.1%, the curves of different fiber lengths are only slightly different so that the effect of fiber length on carbonation is not obvious. From Fig. 4b and c, however, the specimens with fiber length of 6 mm nearly have the strongest carbonation resistance for the same carbonation time but different fiber content.

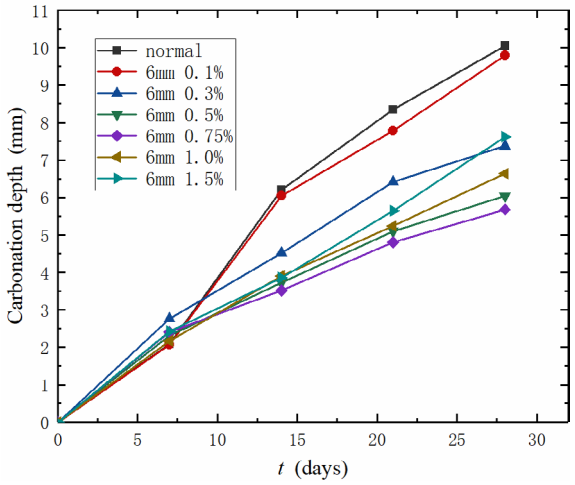


(a) 6 mm

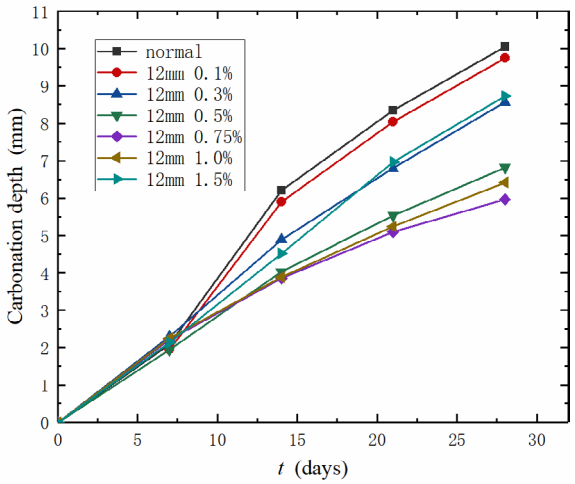


(b) 12 mm

**Fig. 3** Time evolution of carbonation depth in the PVA fiber concrete with fiber lengths of 6 mm and 12 mm.

This suggests that the fiber length should also be selected appropriately.

This should be because the increase in the fracture resistance of PVA fiber concrete comes from the bridging action of fibers across cracks (Zhang & Yang, 2019). If the fibers are too short, their bridging action and ability to inhibit early cracking of concrete would be very limited. If the fibers are too long, however, they can be easily twisted and bent during the concrete-making process. As a result, the bridging action of PVA fibers and the fracture resistance of PVA fiber concrete would also be reduced.

Based on Fick's second law, some theoretical or empirical models were proposed for the carbonation of normal concrete (Czarnecki & Woyciechowski, 2015; Jiang et al., 2000, 2019; Neves et al., 2013; Papadakis, 2000; Wang et al., 2018). It was believed that the carbonation depth is directly proportional to the square roots of the carbon dioxide concentration in the environment and the carbonation time (Czarnecki & Woyciechowski, 2015):

$$d = K\sqrt{C_0 t}, \tag{1}$$

where $d$ is the carbonation depth in unit of mm, $C_0$ is the carbon dioxide concentration in the environment, $t$ is the carbonation time in unit of day, and $K$ is the carbonation coefficient in unit of mm/$\sqrt{\text{day}}$. According to the experimental data, $K$ is fitted. For normal concrete, $K$=3.839 mm/$\sqrt{\text{day}}$. For PVA fiber concrete, however, $K$ can be taken as the linear or quadratic function of the fiber length $x_1$ in unit of mm and fiber volume content $x_2$.

For the linear model,

$$\mathrm{K} = 3.839 + a_1 x_1 + a_2 x_2. \tag{2}$$

But for the quadratic model,

$$K = 3.839 + a_1 x_1 + a_2 x_2 + a_3 x_1^2 + a_4 x_2^2. \tag{3}$$

They have the same constant term as the carbonation coefficient of normal concrete.

The multiple regression analyses were carried out at the significance level of 0.05 to fit the model coefficients in Eqs. (2) and (3), as shown in Table 6. In this table, $R^2$ is the coefficient of determination. It is much lower than 1 for the linear model, but reaches 0.943 for the quadratic model.

According to the linear and quadratic models, the relationship of the carbonation coefficient with the fiber length and content can be expressed as:

$$K = 3.839 - 0.0219x_1 - 0.9500x_2, \tag{4}$$

$$K = 3.839 + 0.0111x_1 - 3.5231x_2 + 0.0005x_1^2 + 1.9239x_2^2. \tag{5}$$

By substituting them into Eq. (1), respectively, two time evolution models of the carbonation depth are obtained for PVA fiber concrete:

$$d = (3.839 - 0.0219x_1 - 0.9500x_2)\sqrt{C_0 t}, \tag{6}$$

$$d = (3.839 + 0.0111x_1 - 3.5231x_2 + 0.0005x_1^2 + 1.9239x_2^2)\sqrt{C_0 t}. \tag{7}$$

As an example, Fig. 5 shows their prediction curves of the carbonation depth of PVA fiber concrete with PVA fiber content of 0.5% and lengths of 3 mm, 6 mm, 12 mm and 18 mm, respectively. It is very clear by comparison

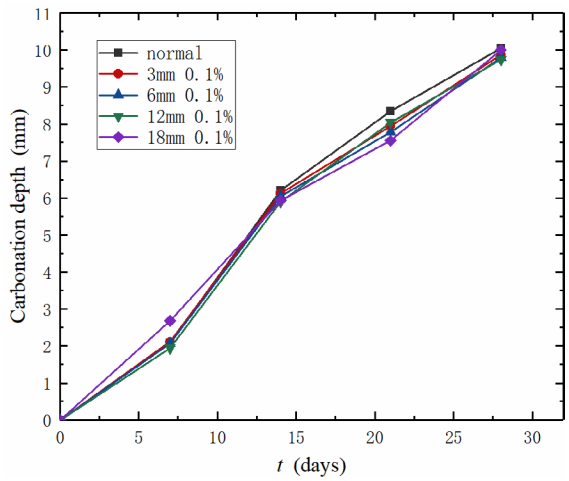


(a) 0.1%

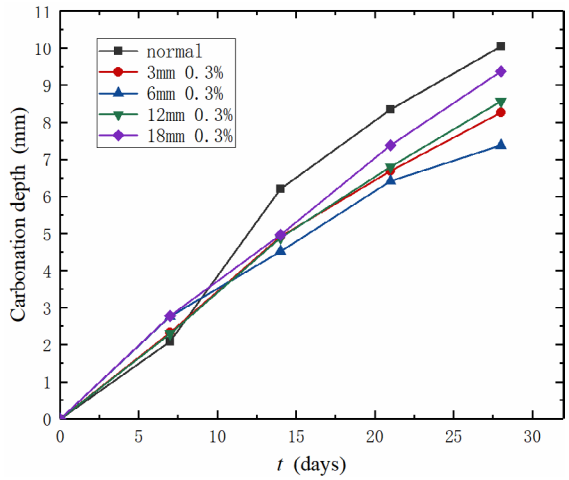


(b) 0.3%

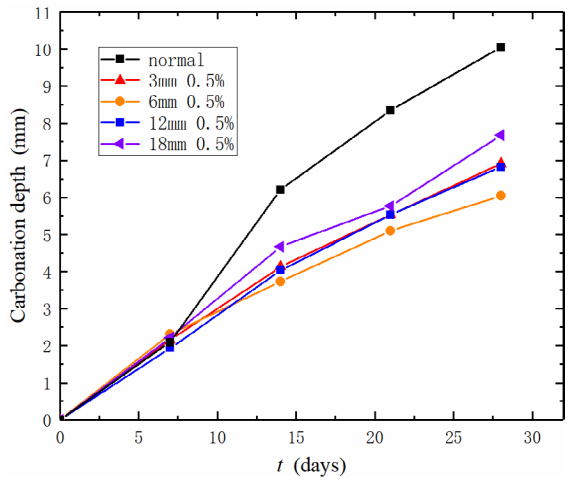


(c) 0.5%

**Fig. 4** Time evolution of carbonation depth in PVA fiber concrete with fiber contents of 0.1%, 0.3% and 0.5%.

that, although both the two model predictions have a certain deviation from the experimental results, the quadratic model has smaller coefficient of determinations and higher fitting accuracy than the linear model. Accordingly, it is more reasonable and was used in the subsequent numerical simulations of carbonation.

### 3.2 Carbon Dioxide Diffusion Equation

The diffusion behavior of carbon dioxide in concrete is driven by its concentration gradient. The governing equation of carbon dioxide concentration in concrete can be expressed as (Liu et al., 2020):

$$\frac{\partial C}{\partial t} = D\nabla^2 C - r, \tag{8}$$

in which $C$ is the carbon dioxide concentration in concrete, $D$ is the diffusion coefficient and $r$ is the carbonation reaction rate. The first term on the right side of Eq. (8) reflects the physical process of carbon dioxide diffusion into the concrete, and the second term is for the carbonation reaction between carbon dioxide and alkaline aggregates. The PVA fibers incorporated into concrete inhibit the diffusion process of carbon dioxide, thus reducing the diffusion coefficient. However, they have little influence on the carbonation reaction, so their influence on the carbonation reaction rate $r$ can be ignored.

By introducing a PVA fiber influence factor $F_4(x_1, x_2)$, the diffusion coefficient for PVA fiber concrete can be expressed as (AL-Ameeri et al., 2021; Hwang et al., 2020; Saetta & Vitaliani, 2004):

$$D = D_0 F_1(T) F_2(H) F_3(\eta) F_4(x_1, x_2), \tag{9}$$

in which $D_0$ is the diffusivity of carbon dioxide in the standard temperature and humidity condition:

$$D_0 = 8 \times 10^{-7}(w/c - 0.34)(1 - \overline{H})^{2.2}, \tag{10}$$

where $w/c$ is the water–cement ratio and $\overline{H}$ is the relative humidity inside the concrete.

In Eq. (9), $F_1(T)$ reflects the influence of temperature on the diffusion coefficient and can be expressed as (Saettaa & Vitaliani, 2004):

$$F_1(T) = \exp\left[\frac{Q}{R}\left(\frac{1}{T_0} - \frac{1}{T}\right)\right], \tag{11}$$

where $Q$=21,800 J/mol is the energy dissipated by the reaction of 1 mol carbon dioxide, $R$=8.314 J/mol·K is the

**Table 6** Multiple regression coefficients.

| Coefficients | $a_1$ | $a_2$ | $a_3$ | $a_4$ | $R^2$ |
|---|---|---|---|---|---|
| Linear model | − 0.0219 | − 0.9500 | | | 0.062 |
| Quadratic model | 0.0111 | − 3.5231 | 0.0005 | 1.9239 | 0.943 |

where $H$ is the ambient humidity.

$F_3(\eta)$ reflects the effect of carbonation degree on the diffusion coefficient and satisfies (Saettaa & Vitaliani, 2004):

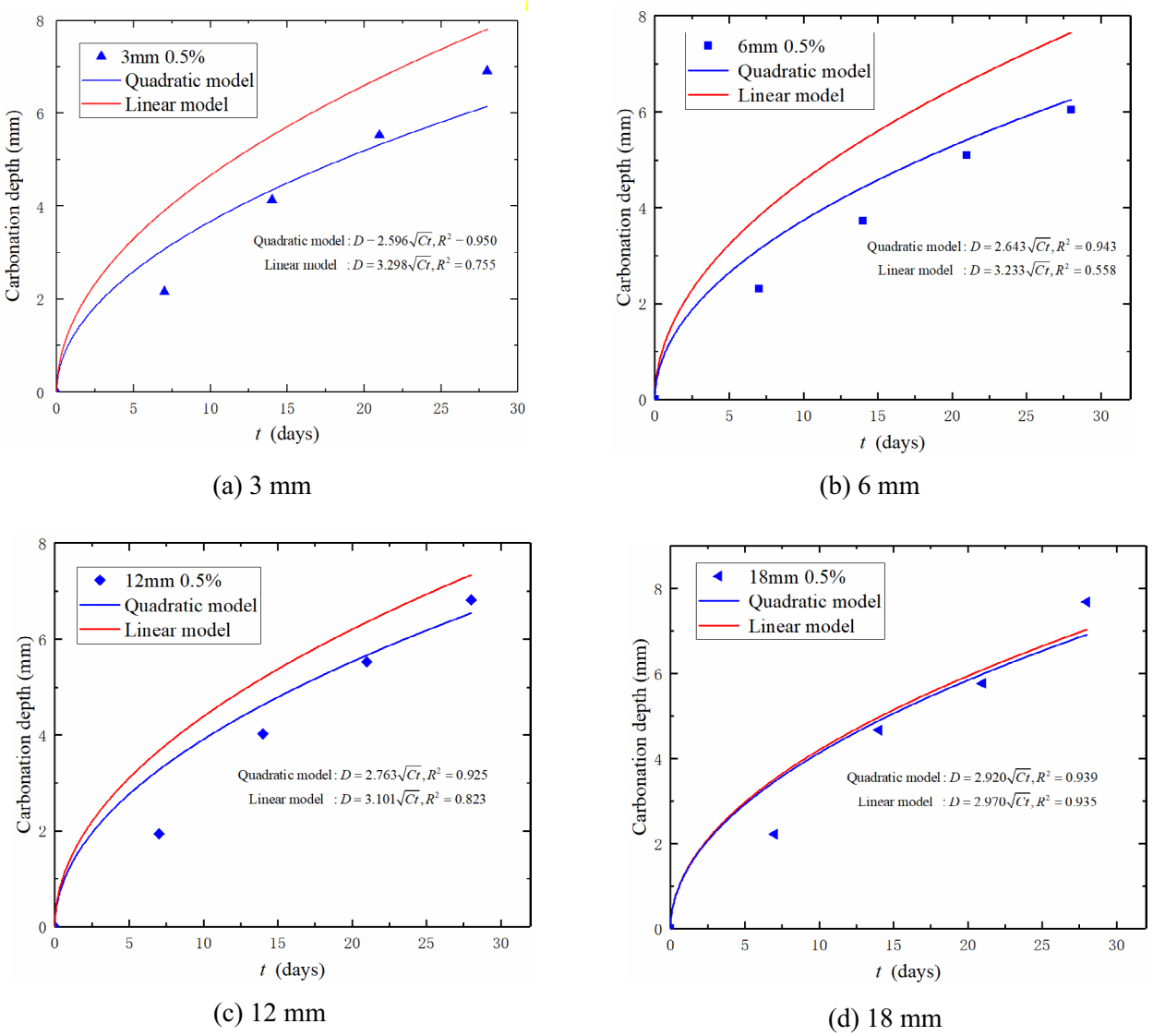


**Fig. 5** Carbonation depth predictions of PVA fiber concrete with a fiber content of 0.5% and different fiber lengths from the linear and quadratic models.

molar gas constant, $T$ is the ambient temperature, and $T_0$ is the reference temperature for measuring $D_0$.

$F_2(H)$ reflects the influence of humidity on the diffusion coefficient and has (Saettaa & Vitaliani, 2004):

$$F_2(H)=(1-H)^{2.5}, \tag{12}$$

$$F_3(\eta)=\begin{cases} 1-\frac{5}{9}\eta & 0\le\eta<0.9 \\ 0.5 & 0.9\le\eta\le 1.0 \end{cases}, \tag{13}$$

where $\eta$ is the carbonation degree. When the concrete is not carbonized, $\eta=0$, but when it is completely carbonized, $\eta=1$.

As the PVA fiber influence factor, $F_4(x_1, x_2)$ reflects the influence of added PVA fiber on the diffusion coefficient and is defined as

$$F_4(x_1, x_2) = \frac{K(x_1, x_2)}{K_0}, \tag{14}$$

where $K(x_1, x_2)$ is the carbonation coefficient of PVA fiber concrete, which can be determined by Eq. (5), and $K_0=3.839\ \text{mm}/\sqrt{\text{day}}$ is the carbonation coefficient of normal concrete.

The carbonation reaction rate $r$ can be expressed as (Saetta & Vitaliani, 2004):

$$r = r_0 \cdot f_1(T) \cdot f_2(H) \cdot f_3(\eta), \tag{15}$$

where $r_0=2.8\times10^{-7}$/s·mol is the carbonation reaction rate in the standard temperature and humidity condition.

$f_1(T)$ reflects the effect of temperature on the carbonation reaction rate:

$$f_1(T) = \exp\left(-\frac{E_0}{RT}\right), \tag{16}$$

where $E_0=91.52$ kJ/mol is the carbonation activation energy.

$f_2(H)$ reflects the influence of humidity on the carbonation reaction rate and is expressed as:

$$f_2(H) = \begin{cases} 0 & 0 \le H < 0.5 \\ 2.5(H-0.5) & 0.5 \le H < 0.9 \\ 1 & 0.9 \le H < 1 \end{cases} \tag{17}$$

$f_3(\eta)$ reflects the effect of carbonation degree on the carbonation reaction rate:

$$f_3(\eta)=1-\eta. \tag{18}$$

The molecular concentration of carbon dioxide in the environment, $C_\text{m}$, is given by the ideal gas equation:

$$C_\text{m} = \frac{PV}{RT}, \tag{19}$$

in which the pressure is expressed as $P=101325\,C_\text{V}$ in unit of Pa with $C_\text{V}$ as the volume ratio of carbon dioxide in the air, and $V$ is the gas volume.

According to the relative molecular mass of carbon dioxide, $C_\text{m}$ can be converted to the mass concentration of carbon dioxide at the boundary $C_0$ by

$$C_0 = 0.044C_\text{m}. \tag{20}$$

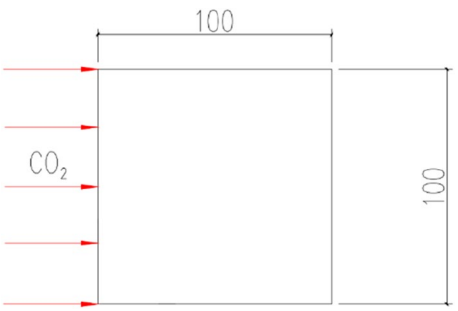


**Fig. 6** Two-dimensional model of an experimental sample (size unit: mm).

## 4 Model Validation

The carbonation reaction reduces the pH value when carbon dioxide penetrates into the concrete. The concentration of carbon dioxide gradually decreases from outside to inside in the concrete. In general, there is pH value greater than 10.0 and lower carbon dioxide concentration in the uncarbonized zone, but there is pH value less than 10.0 and higher carbon dioxide concentration in the carbonation zone. The lowest pH value for phenolphthalein color development is about 10.0 (Ji et al., 2014). Therefore, the measured carbonation depth value for the color boundary of phenolphthalein reagent or the carbonation front in concrete corresponds to the critical carbon dioxide concentration. If the carbon dioxide concentration exceeds this critical value, the concrete would be carbonized. Otherwise, the concrete would not be carbonized.

In addition, the critical carbon dioxide concentration can also be determined by simulating the carbon dioxide concentration distribution in the concrete under the condition of laboratory with ANSYS software. According to the specimen size in Sect. 3.1, a two-dimensional model with a size of 100 mm × 100 mm is established, as shown in Fig. 6. Carbon dioxide can diffuse into the sample only from the left side of the model. According to the experimental condition, the concentration of carbon dioxide on the left outside is 20% and the ambient temperature is 20 ℃. The concrete is assumed uniform and isotropic. In the carbonation experiments in Sect. 3.1, the carbonation depth of the normal concrete specimen is 10.05 mm after 28-day carbonation. According to the numerical results obtained by solving Eq. (8), there is the critical carbon dioxide concentration of 0.262 kg/m$^3$ in this position.

Subsequently, the carbon dioxide concentration distributions in the concrete models with different PVA fiber contents and lengths are further simulated for different carbonation time. Their carbonation depth values are determined according to the critical carbon dioxide concentration. By comparing the experimental and

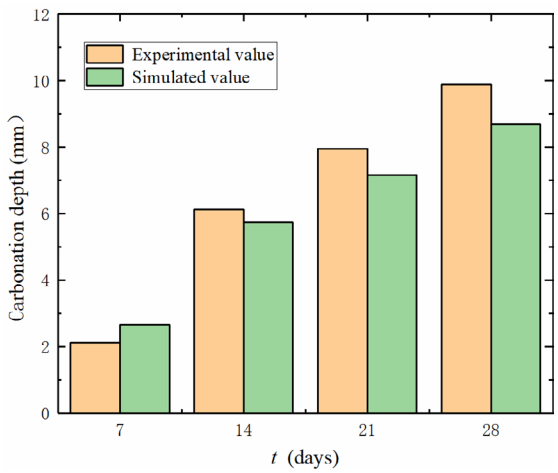


(a) 0.1% PVA content

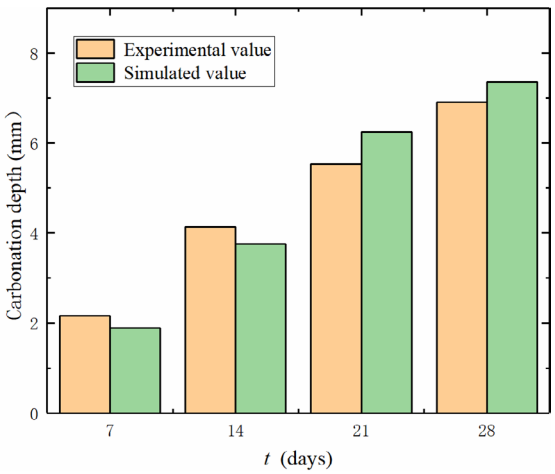


(b) 0.5% PVA content

**Fig. 7** Comparison between the simulated and experimental carbonation depth values of PVA fiber concrete with 3 mm fiber length and different contents.

numerical results, the model and numerical method are validated.

Fig. 7 shows the experimental and numerical carbonation depth values of PVA fiber concrete specimens with 3 mm PVA fiber length and 0.1% or 0.5% content for different carbonation ages. It can be seen that for different fiber contents and different carbonation ages, the numerical results are quite close to the experimental ones. For the specimens carbonized for 28 days, the average error of carbonation depth is about 1.95%. Taking the PVA fiber concrete with a length of 3 mm and a content of 0.5% as an example, according to the carbon dioxide concentration distribution inside the specimen after 28-day carbonation, the carbonation depth is 7.36 mm. On the other hand, its averaged experimental carbonation depth is 6.91 mm. The error between the two is about 6%. This shows that the carbon dioxide diffusion equation with the determined coefficient is reasonable and acceptable.

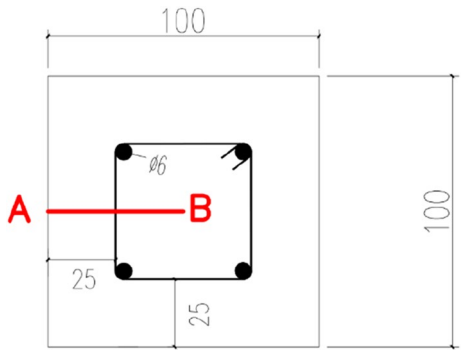


**Fig. 8** Reinforced concrete component with a rectangular section (size unit: mm).

## 5 Simple Application to Carbonation Prediction of Reinforced Concrete Components

### 5.1 Geometric Model

As a simple application, the carbonation behavior of a reinforced concrete component with a rectangular cross-section is simulated at 20% ambient carbon dioxide concentration and 20 ℃ ambient temperature by solving Eq. (8) with the aid of ANSYS software. Its section size is 100 mm × 100 mm, as shown in Fig. 8. Four longitudinal reinforcements are round steel bars with a radius of 3 mm. The protective layer has a thickness of 25 mm. Carbon dioxide diffuses into the component from all sides.

### 5.2 Results and Analysis

On the line between the midpoint A on the left side of the rectangular section and the centroid of the section B, marked by the red line segment in Fig. 8, four points 3 mm, 5 mm, 10 mm and 15 mm away from point A are selected as the observation points of carbon dioxide concentration. From the numerical results, their carbon dioxide concentration values after 7-, 14- and 28-day carbonation are extracted, respectively, as shown in Fig. 9.

It can be seen that the carbon dioxide concentration on the surface of the component remains unchanged at 0.36 kg/m$^3$. After certain carbonation time, the curve of carbon dioxide concentration with the depth shows a downward trend along the observed path, and the downward trend is slowed down with the increase of carbonation age. This shows that the deeper into the surface of the component, the lower the carbon dioxide

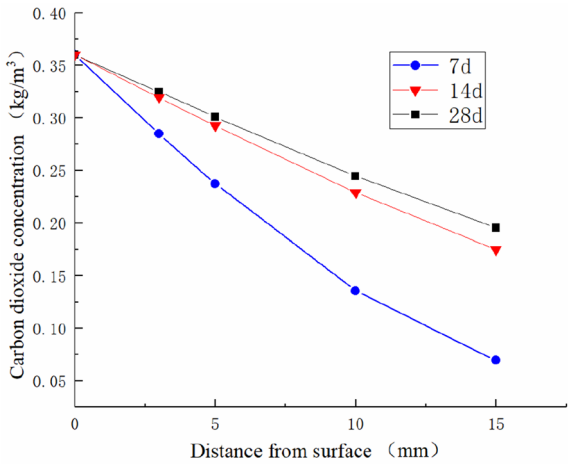


**Fig. 9** Variations of carbon dioxide concentration with the depth for different carbonation ages.

concentration. In addition, the longer the carbonation lasts, the flatter the curve of carbon dioxide concentration is. With the extension of carbonation time, the more fully carbon dioxide diffuses into the component interior, the less the decrease of its concentration with the depth.

In Sect. 3.1, it is concluded that the PVA fiber concrete with 6 mm fiber length and 0.75% volume content has the best carbonation resistance. To vividly show the diffusion process of carbon dioxide inside the concrete, Figs. 10 and 11 show the contours of carbon dioxide concentration in the rectangular-section reinforced concrete components made from normal concrete and PVA fiber concrete with 6 mm fiber length and 0.75% volume content after suffering carbonation of 7, 14, 21 and 28 days, respectively. The ranges of carbon dioxide concentration represented by different colors are fixed for comparison. It can be seen that, with the growth of carbonation age, the red area with high carbon dioxide concentration keeps expanding, while the blue area with low carbon

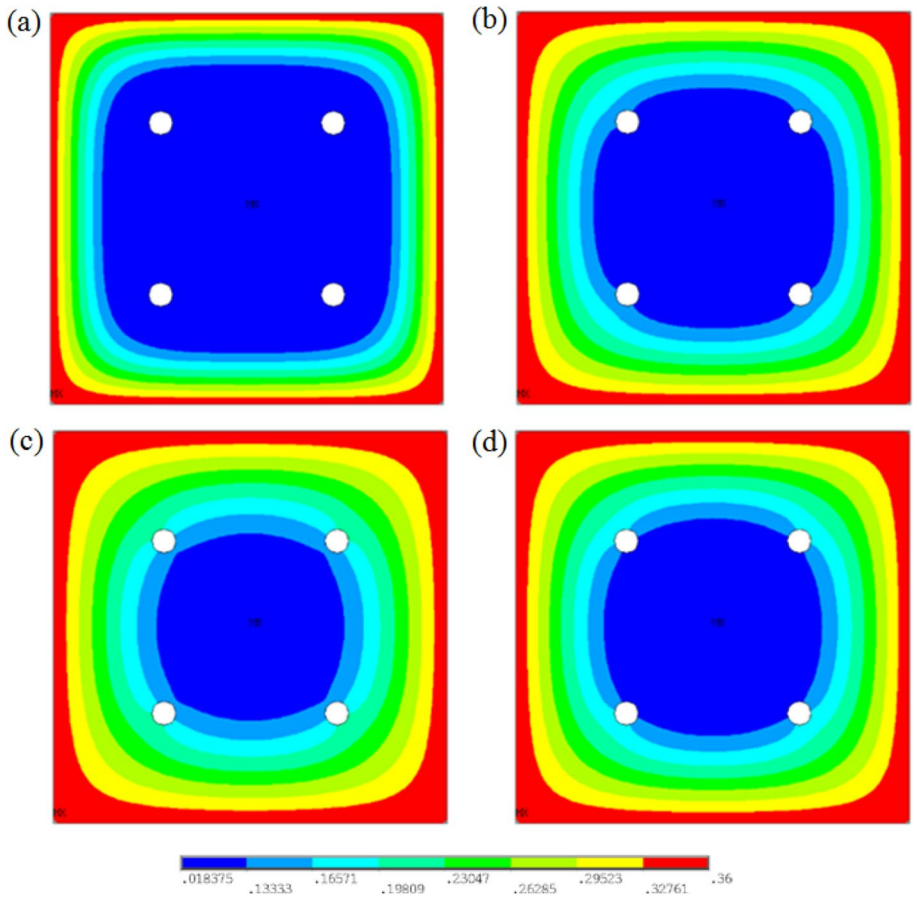


**Fig. 10** Contours of carbon dioxide concentration in the normal concrete component: **a** for 7 days, **b** for 14 days, **c** for 21 days, and **d** for 28 days.

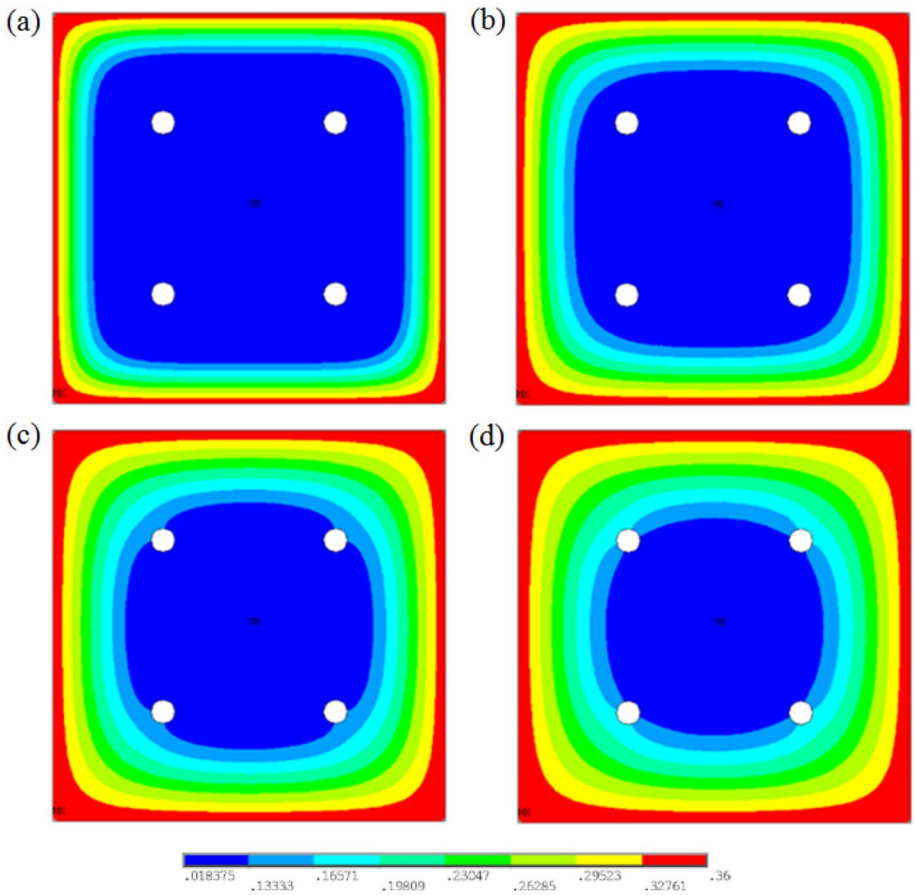


**Fig. 11** Contours of carbon dioxide concentration in the 0.75% PVA fiber concrete component with 6 mm length: **a** for 7 days, **b** for 14 days, **c** for 21 days, and **d** for 28 days.

dioxide concentration keeps shrinking obviously, which reflects the continuous diffusion of carbon dioxide from surface to interior. In addition, by comparing the carbonation contours of the normal concrete and PVA fiber concrete components, it can be found that, for the same carbonation age, the red area of PVA fiber concrete is obviously smaller than that of normal concrete, while its blue area is obviously larger than that of normal concrete. This fully shows that compared with the normal concrete, the PVA fiber concrete has stronger resistance to carbon dioxide diffusion.

### 5.3 Durability and Carbonation Life

The damage of carbonation to the durability of reinforced concrete lies in the depassivation of the internal reinforcement after carbon dioxide penetrates the protective layer of reinforced concrete, as well as the vicious circle from steel corrosion to surface burst and corrosion intensification. As a result, the structural carrying capacity continuously declines. Therefore, the diffusion of carbon dioxide in the concrete structures is closely related to their durability.

The carbonation depth criterion (Marques et al., 2013; Sun et al., 2020) can be used to study the carbonation life of PVA fiber concrete component. According to this criterion, when carbon dioxide diffuses to the steel bar surface, the concrete protective layer would be completely destroyed and the steel bar begins to rust. In the following, the numerical simulation method is firstly adopted to obtain the time required for the carbon dioxide concentration to reach 0.262 kg/m$^3$ at the depth of 25 mm from the surface, which is the protective layer thickness of the reinforcements. This is the carbonation life of the concrete component under the accelerated carbonation experiment condition. Then, the carbonation life of the component under the natural environment is obtained by the following empirical relation, so as to realize the prediction of the carbonation life or durability under the natural environment (Liu et al., 2020):

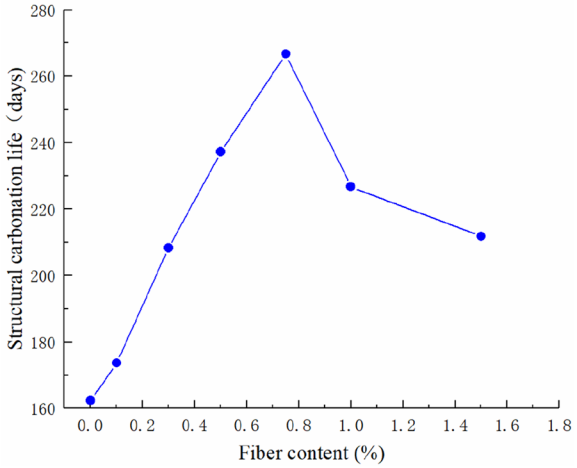


**Fig. 12** Carbonation life versus fiber content for the 6 mm length PVA fiber concrete component under the accelerated carbonation experiment condition.

$$\frac{d_2}{d_1}=\sqrt{\frac{t_2\cdot c_2}{t_1\cdot c_1}}, \tag{21}$$

in which, $d_1$ is the carbonation depth under the accelerated carbonation experiment condition, $d_2$ is the carbonation depth under the natural condition, $t_1$ is the accelerated carbonation time, $t_2$ is the natural carbonation time, $c_1$ is the carbon dioxide concentration for the accelerated experiment, namely 20% here, and $c_2$ is the carbon dioxide concentration in the natural environment, namely 0.03%.

Fig. 12 shows the predicted carbonation life of the PVA fiber concrete component with a fiber length of 6 mm and a volume content of fiber increased from 0 to 1.5% under the accelerated carbonation experiment condition. It can be seen that compared with the reinforced normal concrete component without PVA fibers, the carbonation life is significantly improved. The carbonation life of reinforced normal concrete component is about 162.3 days, but after adding 6 mm length and 0.75% volume content PVA fibers, the carbonation life reaches about 266.7 days. The life is extended about 39.15%. However, it must be noted that more PVA fiber content is not better. The carbonation life increases monotonically when the PVA fiber content increases from 0 to 0.75%, but decreases monotonically when the content continues to increase from 0.75% to 1.5%. Therefore, the carbonation life reaches the maximum at the PVA fiber content of about 0.75%.

According to Eq. (21), the carbonation life of the reinforced normal concrete component in the natural environment is about 228 years. This is a surprising result. However, it is consistent with that from Jiang et al. (2010), in which it takes about 150 years for normal concrete to reach carbonation depth of 17 mm in the natural environment. It was believed that the carbonation life of concrete would be significantly reduced due to other factors, such as fatigue loading.

Due to the addition of 6 mm length and 0.75% volume PVA fibers, the carbonation life of reinforced concrete component in the natural environment is up to 111.7 years. Compared with normal concrete, it is extended about 150 years. This indicates that adding PVA fiber into concrete can protect the reinforcement better, delay the carbonation life of reinforced concrete significantly, and improve the durability.

## 6 Conclusions

In this paper, the influences of fiber length and volume content on the carbonation behavior of PVA fiber concrete are investigated by the accelerated carbonation experiments and numerical simulations. The following conclusions are drawn:

(1) The carbonation resistance of concrete can be remarkably improved by the appropriate addition of PVA fibers. Both the length and volume content of PVA fibers have important influences on the carbonation development of concrete. With the increase of fiber length or content, the carbonation resistance of concrete tends to be strengthened first and then weakened. When the fiber length is 6 mm and the fiber content is about 0.75%, the carbonation resistance of concrete is the strongest.

(2) The carbonation coefficient can be regarded as a function of the PVA fiber length and content, and their relationship can be better described by the quadratic function model than by the linear model. Based on this relation, the coefficient of the carbon dioxide diffusion equation can also be determined by introducing the PVA fiber influence factor involving the PVA fiber length and content effects.

(3) The durability of reinforced concrete components can be significantly improved by appropriately adding PVA fibers. In the accelerated carbonation experiment condition, the PVA fiber concrete component with 6 mm length and 0.75% volume content has the longest carbonation life. Compared with the reinforced normal concrete component, the carbonation life of reinforced concrete component with PVA fibers of 6 mm length and 0.75% volume content in the natural environment is extended about 65.8%.

**Acknowledgements**
Not applicable.

**Authors' contributions**
ZL: writing the manuscript, experimental works, analyzing data. XY: conceptualization, project administration, funding acquisition, reviewing, editing. HJ: experimental works, analyzing data. CZ: methodology, review and comments. All authors read and approved the final manuscript.

**Authors' information**
Zuyun Luo is a graduated Master student from the School of Aerospace Engineering, Huazhong University of Science and Technology, Wuhan, China and also a civil engineer from the China Railway Siyuan Survey and Design Group Co., Ltd.
Chuanchuan Zhang is a senior engineer from Shanxi Transportation Technology Research & Development Co., Ltd., Taiyuan.
Xinhua Yang is a professor from the School of Aerospace Engineering, Huazhong University of Science and Technology, Wuhan, China.
Heli Ji is a graduated Master student from the School of Aerospace Engineering, Huazhong University of Science and Technology, Wuhan, China.

**Funding**
This work was supported by the National Natural Science Foundation of China (Grant Nos 11832013 and 12072120) and Basic Apply Research Program of Shanxi Province (No. 201901D211533).

**Availability of data and materials**
The data sets used and/or analyzed during the current study are available from the corresponding author on reasonable request.

## Declarations

**Competing interests**
The authors declare that they have no competing interests.

**Author details**
[1]School of Aerospace Engineering, Huazhong University of Science and Technology, Wuhan 430074, China. [2]China Railway Siyuan Survey and Design Group Co., Ltd., Wuhan 430063, China. [3]Shanxi Transportation Technology Research and Development Co., Ltd., Taiyuan 030032, China.

Received: 13 September 2021 Accepted: 21 January 2022
Published online: 08 February 2022

**References**

AL-Ameeri, A. S., et al. (2021). Impact of climate change on the carbonation in concrete due to carbon dioxide ingress: Experimental investigation and modelling. *Journal of Building Engineering, 44*, 102594.
Aminul Haque, M., Chen, B., Ahmad, M. R., & Shah, S. F. A. (2019). Evaluating the physical and strength properties of fibre reinforced magnesium phosphate cement mortar considering mass loss. *Construction and Building Materials, 217*, 427–440.
An, X., Wu, Q., Jin, F., Huang, M., Zhou, H., Chen, C., et al. (2014). Rock-filled concrete, the new norm of SCC in hydraulic engineering in China. *Cement and Concrete Composites, 54*, 89–99.
Belletti, B., Cerioni, R., Meda, A., & Plizzari, G. (2008). Design aspects on steel fiber-reinforced concrete pavements. *Journal of Materials in Civil Engineering, 20*(9), 599–607.
Carević, V., & Ignjatović, I. (2019). Influence of loading cracks on the carbonation resistance of RC elements. *Construction and Building Materials, 227*, 116583.
Chen, J., & Qian, C. (2017). Loading history dependence of retardation time of calcium-silicate-hydrate. *Construction and Building Materials, 147*, 558–565.
Chen, X., Shi, X., Zhou, J., Chen, Q., Li, E., & Du, X. (2018). Compressive behavior and microstructural properties of tailings polypropylene fibre-reinforced cemented paste backfill. *Construction and Building Materials, 190*, 211–221.
Chen, X., Wan, D., Jin, L., Qian, K., & Fu, F. (2019). Experimental studies and microstructure analysis for ultra high-performance reactive powder concrete. *Construction and Building Materials., 229*, 116924.
Czarnecki, L., & Woyciechowski, P. (2015). Modelling of concrete carbonation; is it a process unlimited in time and restricted in space? *Bulletin of the Polish Academy of Sciences Technical Sciences, 63*(1), 43–54.
de la Fuente, A., Escariz, R. C., de Figueiredo, A. D., Molins, C., & Aguado, A. (2012). A new design method for steel fibre reinforced concrete pipes. *Construction and Building Materials, 30*, 547–555.
Ding, H., & Chen, J. (2019). Research on the resistivity attenuation law of cementitious conductive composites induced by stress relaxation. *Construction and Building Materials, 206*, 347–354.
Felix, E. F., Carrazedo, R., & Possan, E. (2021). Carbonation model for fly ash concrete based on artificial neural network: Development and parametric analysis. *Construction and Building Materials, 266*, 121050.
Flores Medina, N., Barluenga, G., & Hernández-Olivares, F. (2014). Enhancement of durability of concrete composites containing natural pozzolans blended cement through the use of Polypropylene fibers. *Composites Part B: Engineering, 61*, 214–221.
Flores Medina, N., Barluenga, G., & Hernández-Olivares, F. (2015). Combined effect of polypropylene fibers and silica fume to improve the durability of concrete with natural Pozzolans blended cement. *Construction and Building Materials, 96*, 556–566.
Frazão, C., Camões, A., Barros, J., & Gonçalves, D. (2015). Durability of steel fiber reinforced self-compacting concrete. *Construction and Building Materials, 80*, 155–166.
Han, J., Liu, W., Wang, S., Du, D., Xu, F., Li, W., et al. (2016). Effects of crack and ITZ and aggregate on carbonation penetration based on 3D micro X-ray CT microstructure evolution. *Construction and Building Materials, 128*, 256–271.
Hwang, J., Kwak, H., & Shim, M. (2020). Numerical approach for concrete carbonation considering moisture diffusion. *Materials and Structures*. https://doi.org/10.1617/s11527-020-01550-4
Ji, Y., Wu, M., Ding, B., et al. (2014). The experimental investigation of width of semi-carbonation zone in carbonated concrete. *Construction and Building Materials, 65*, 67–75.
Jiang, J. Y., Sun, W., Jin, Z. Q., et al. (2010). Service life prediction of structural concrete under coupled interactions of fatigue loading and carbonation factor. *Journal of Building Materials, 13*(3), 304–309. (in Chinese).
Jiang, L., Lin, B., & Cai, Y. (2000). A model for predicting carbonation of high-volume fly ash concrete. *Cement and Concrete Research, 30*(5), 699–702.
Jiang, Z., Gu, X., Huang, Q., & Zhang, W. (2019). Statistical analysis of concrete carbonation depths considering different coarse aggregate shapes. *Construction and Building Materials, 229*, 116856.
Li, D., Li, L., & Wang, X. (2020). Mathematical modelling of concrete carbonation with moving boundary. *International Communications in Heat and Mass Transfer, 117*, 104809.
Li, L., & Cao, M. (2018). Influence of calcium carbonate whisker and polyvinyl alcohol–steel hybrid fiber on ultrasonic velocity and resonant frequency of cementitious composites. *Construction and Building Materials, 188*, 737–746.
Liu, P., Yu, Z., & Chen, Y. (2020). Carbonation depth model and carbonated acceleration rate of concrete under different environment. *Cement and Concrete Composites, 114*, 103736.
Marques, P. F., Chastre, C., & Nunes, Â. (2013). Carbonation service life modelling of RC structures for concrete with Portland and blended cements. *Cement and Concrete Composites, 37*, 171–184.
Mi, R., Pan, G., & Shen, Q. (2019). Carbonation modelling for cement-based materials considering influences of aggregate and interfacial transition zone. *Construction and Building Materials, 229*, 116925.
Muntean, R., Cazacu, C., Mizgan, P., Galatanu, T., & Tamas, F. (2017). Practical applications of dispersely reinforced concrete with polypropylene fibers: Beams. *Procedia Engineering, 181*, 285–292.
Neves, R., Branco, F., & de Brito, J. (2013). Field assessment of the relationship between natural and accelerated concrete carbonation resistance. *Cement and Concrete Composites, 41*, 9–15.
Omikrine Metalssi, O., Aït-Mokhtar, A., & Turcry, P. (2020). A proposed modelling of coupling carbonation-porosity-moisture transfer in concrete based on mass balance equilibrium. *Construction and Building Materials, 230*, 116997.

Pacheco-Torgal, F., Abdollahnejad, Z., Miraldo, S., Baklouti, S., & Ding, Y. (2012). An overview on the potential of geopolymers for concrete infrastructure rehabilitation. *Construction and Building Materials, 36*, 1053–1058.
Papadakis, V. G. (2000). Effect of supplementary cementing materials on concrete resistance against carbonation and chloride ingress. *Cement and Concrete Research, 30*(2), 291–299.
Possan, E., Felix, E. F., & Thomaz, W. A. (2016). CO2 uptake by carbonation of concrete during life cycle of building structures. *Journal of Building Pathology and Rehabilitation*. https://doi.org/10.1007/s41024-016-0010-9
Razmi, A., & Mirsayar, M. M. (2017). On the mixed mode I/II fracture properties of jute fiber-reinforced concrete. *Construction and Building Materials, 148*, 512–520.
Saetta, A. V., Schrefler, B. A., & Vitaliani, R. V. (1993). The carbonation of concrete and the mechanism of moisture, heat and carbon dioxide flow through porous materials. *Cement and Concrete Research, 23*(4), 761–772.
Saetta, A. V., & Vitaliani, R. V. (2004). Experimental investigation and numerical modeling of carbonation process in reinforced concrete structures. *Cement and Concrete Research, 34*(4), 571–579.
Saettaa, A. V., & Vitaliani, R. V. (2004). Experimental investigation and numerical modeling of carbonation process in reinforced concrete structures. Part I: Theoretical formulation. *Cement and Concrete Research, 34*, 571–579.
Samarakkody, D. I., Thambiratnam, D. P., Chan, T. H. T., & Moragaspitiya, P. H. N. (2017). Differential axial shortening and its effects in high rise buildings with composite concrete filled tube columns. *Construction and Building Materials, 143*, 659–672.
Spelter, A., Bergmann, S., Bielak, J., & Hegger, J. (2019). Long-term durability of carbon-reinforced concrete: An overview and experimental investigations. *Applied Sciences, 9*(8), 1651.
Sun, B., Xiao, R., Ruan, W., & Wang, P. (2020). Corrosion-induced cracking fragility of RC bridge with improved concrete carbonation and steel reinforcement corrosion models. *Engineering Structures, 208*, 110313.
The state standard of the People's Republic of China: Standard test for methods of long-term performance and durability of ordinary concrete (GBT50082–2009), China Building Industry Press, 2009 **(in Chinese)**.
Thong, C. C., Teo, D. C. L., & Ng, C. K. (2016). Application of polyvinyl alcohol (PVA) in cement-based composite materials: A review of its engineering properties and microstructure behavior. *Construction and Building Materials, 107*, 172–180.
Tiberti, G., Germano, F., Mudadu, A., & Plizzari, G. A. (2018). An overview of the flexural post-cracking behavior of steel fiber reinforced concrete. *Structural Concrete, 19*(3), 695–718.
Tonoli, G. H. D., Carmello, G. F., Fioroni, C. A., Pereira, T. D. L., Rocha, G., Souza, R. B. D., et al. (2019). Influence of the initial moisture content on the carbonation degree and performance of fiber-cement composites. *Construction and Building Materials, 215*, 22–29.
Wang, J., Su, H., & Du, J. (2018). Influence of coupled effects between flexural tensile stress and carbonation time on the carbonation depth of concrete. *Construction and Building Materials, 190*, 439–451.
WSNB Dong Cui. (2018). Use of tomography to understand the influence of preconditioning on carbonation tests in cement-based materials. *Cement and Concrete Composites, 88*, 52–63.
Xu, H., Shao, Z., Wang, Z., Cai, L., Li, Z., Jin, H., et al. (2020). Experimental study on mechanical properties of fiber reinforced concrete: Effect of cellulose fiber, polyvinyl alcohol fiber and polyolefin fiber. *Construction and Building Materials, 261*, 120610.
Zhang, C., & Yang, X. (2019). Bilinear elastoplastic constitutive model with polyvinyl alcohol content for strain-hardening cementitious composite. *Construction and Building Materials, 209*, 388–394.
Zhang, W., Yin, C., Ma, F., Huang, Z., et al. (2018). Mechanical properties and carbonation durability of engineered cementitious composites reinforced by polypropylene and hydrophilic polyvinyl alcohol fibers. *Materials, 11*, 1147.
Zhu, X. F., & Lv, D. W. (2011). Application and research of high-strength steel fiber reinforced concrete in a project. *Advanced Materials Research, 261–263*, 436–440.

## Publisher's Note